THE JOURNAL OF BIOLOGICAL CHEMISTRY VOL. 291, NO. 16, pp. 8387–8398, April 15, 2016

Explaining the Serological Characteristics of *Streptococcus suis* Serotypes 1 and 1/2 from Their Capsular Polysaccharide Structure and Biosynthesis*[S]

Received for publication, November 4, 2015, and in revised form, February 17, 2016 Published, JBC Papers in Press, February 24, 2016, DOI 10.1074/jbc.M115.700716

Marie-Rose Van Calsteren[‡§], Guillaume Goyette-Desjardins[§¶1], Fleur Gagnon[‡], Masatoshi Okura[‖], Daisuke Takamatsu[‖], René Roy[‡‡], Marcelo Gottschalk[§¶], and Mariela Segura[§¶2]**

*From the [‡]Food Research and Development Centre, Agriculture and Agri-Food Canada, Saint-Hyacinthe, Quebec J2S 8E3, Canada, the [§]Swine and Poultry Infectious Disease Research Centre and [¶]Research Group on Infectious Diseases of Swine, Faculty of Veterinary Medicine, University of Montreal, Saint-Hyacinthe, Quebec J2S 2M2, Canada, the [‖]Bacterial and Parasitic Diseases Research Division, National Institute of Animal Health, National Agriculture and Food Research Organization, Tsukuba, Ibaraki 305 0856, Japan, the **United Graduate School of Veterinary Sciences, Gifu University, Gifu, Gifu 501 1193, Japan, and the [‡‡]Department of Chemistry, Université du Québec à Montréal, Montreal, Quebec H3C 3P8, Canada*

The capsular polysaccharide (CPS) is a major virulence factor in many encapsulated pathogens, as it is the case for *Streptococcus suis*, an important swine pathogen and emerging zoonotic agent. Moreover, the CPS is the antigen at the origin of *S. suis* classification into serotypes. Hence, analyses of the CPS structure are an essential step to dissect its role in virulence and the serological relations between important serotypes. Here, the CPSs of serotypes 1 and 1/2 were purified and characterized for the first time. Chemical and spectroscopic data gave the following repeating unit sequences: [6)[Neu5Ac(α2–6)GalNAc(β1–4)GlcNAc(β1–3)]Gal(β1–3)Gal(β1–4)Glc(β1–]$_n$ (serotype 1) and [4)[Neu5Ac(α2–6)GalNAc(β1–4)GlcNAc(β1–3)]Gal(β1–4)[Gal(α1–3)]Rha(β1–4)Glc(β1–]$_n$ (serotype 1/2). The *Sambucus nigra* lectin, which recognizes the Neu5Ac(α2–6)Gal/GalNAc sequence, showed binding to both CPSs. Compared with previously characterized serotype 14 and 2 CPSs, *N*-acetylgalactosamine replaces galactose as the sugar bearing the sialic acid residue in the side chain. Serological analyses of the cross-reaction of serotype 1/2 with serotypes 1 and 2 and that between serotypes 1 and 14 suggested that the side chain, and more particularly the terminal sialic acid, constitutes one important epitope for serotypes 1/2 and 2. The side chain is also an important serological determinant for serotype 1, yet sialic acid seems to play a limited role. In contrast, the side chain does not seem to be part of a major epitope for serotype 14. These results contribute to the understanding of the relationship between *S. suis* serotypes and provide the basis for improving diagnostic tools.

Streptococcus suis is one of the most important pathogens in the porcine industry causing septicemia, meningitis, and many other infections. It is also an emerging zoonotic pathogen. *S. suis* is a normal inhabitant of the upper respiratory tract of pigs. The biochemical identification of isolates recovered from clinically healthy pigs (mainly from tonsil samples) is difficult to achieve due to the presence of other streptococci that are part of the normal oral microflora and that are phenotypically similar to *S. suis*. For this reason, molecular biology techniques have been developed during the last decade to allow the detection and identification of *S. suis* strains at the species level (1). However, serotyping, which should be a part of the routine identification of *S. suis* strains recovered from diseased pigs and humans, is absolutely required to provide further confirmation regarding the pathogen identity. To date, 35 serotypes have been originally described based on capsular polysaccharide (CPS)[3] antigenic diversity, and most of them have been isolated from diseased pigs (2–5). However, evidence accumulated throughout the years has demonstrated a high level of genetic diversity in the *S. suis* species, leading to the reclassification of several serotypes (such as serotypes 26, 32, and 34) to different species (1). Globally, the top 10 predominant *S. suis* serotypes isolated from clinical cases in pigs are, in decreasing order, serotypes 2, 9, 3, 1/2, 7, 8, 4, 22, 5, and 1, along with around 15% of the strains being non-typable. However, there is a clear geographical effect on the distribution of serotypes (1). In North America, serotypes 2 and 3 are the most prevalent, followed by serotype 1/2 (1). Among virulent serotypes, serotype 2 and, to a lesser extent, serotype 14 are considered serious and high risk emerging zoonotic agents, and their accurate identification is fundamental for diagnostic laboratories.

Proper serological typing must be performed using either a coagglutination test or a capillary precipitation test or with Neufeld's capsular reaction using reference antisera (3, 4). The coagglutination test is preferred by many laboratories, espe-

* This work was supported by Natural Sciences and Engineering Research Council of Canada (NSERC) Grant 342150 (to M. S.). The authors declare that they have no conflicts of interest with the contents of this article.
[S] This article contains supplemental Tables S1 and S2 and Figs. S1–S12.
[1] Recipient of an NSERC fellowship.
[2] To whom correspondence should be addressed: Dept. of Pathology and Microbiology, Faculty of Veterinary Medicine, University of Montreal, Saint-Hyacinthe, Quebec J2S 2M2, Canada. Tel.: 450-773-8521 (ext. 0080); Fax: 450-778-8108; E-mail: mariela.segura@umontreal.ca.

[3] The abbreviations used are: CPS, capsular polysaccharide; DEPT, distortionless enhancement by polarization transfer; DSS, 2,2-dimethyl-2-silapentane-5-sulfonate; ELLA, enzyme-linked lectin assay; HMBC, heteronuclear multiple-bond coherence; HSQC, heteronuclear single-quantum coherence; MLEV, Malcom Levitt's sequence; ROESY, rotating-frame nuclear Overhauser effect spectroscopy; TOCSY, total correlation spectroscopy; T-ROESY, ROESY without TOCSY; Neu, neuraminic acid; Neu5Ac, *N*-acetylneuraminic acid; Rha, rhamnose.

cially in North America (6). Some serotypes cross-react, indicating the presence of common antigenic determinants. This cross-reaction is probably due to similar or closely related structural features of the CPSs. To date, important cross-reactions have been described, including between serotypes 1/2 and 1, serotypes 1/2 and 2, and serotypes 1 and 14 (3, 6, 7). The *cps* loci, in particular the genes encoding putative glycosyltransferases and polymerases, are known for these four serotypes (8). Genetically, the *cps* loci of serotypes 2 and 1/2 are almost identical, and no sequence differences that may contribute to the antigenic divergences have been observed between the two serotypes so far (9). Although the *cps* loci of serotypes 1 and 14 are also almost identical, a putative glycosyltransferase gene (*cps1G*) of the serotype 1 reference strain and a sequenced Chinese strain had a frameshift mutation, whereas the corresponding gene (*cps14G*) of the serotype 14 reference strain and a sequenced Chinese strain was intact. These results implied that the mutation in *cps1G* might contribute to the antigenic differences between serotypes 1 and 14 (9); however, no further analyses have been done to investigate this hypothesis. Indeed, a major drawback in recently developed PCR-based typing systems is the fact that the serotypes 2 and 14 cannot be distinguished from serotypes 1/2 and 1, respectively, since both of these serotype pairs do not possess unique *cps* genes (1, 9).

To understand the important role of the CPS in serotyping and in the interactions of *S. suis* with the host, knowledge regarding the specific structure that confers capsular properties to each individual serotype is necessary. So far, the CPS repeating unit structure has been determined only for serotypes 2 and 14 (10, 11). Our hypothesis is that the structure of serotype 1 CPS is highly similar to that of serotype 14 CPS but somehow different from that of serotype 2 CPS, whereas serotype 1/2 CPS contains structural elements found mainly in serotype 2 CPS and, to a lesser extent, in serotype 1 CPS. Here, the CPSs of serotypes 1 and 1/2 were purified and characterized for the first time. Serological analyses of the cross-reaction of serotype 1/2 with serotypes 1 and 2 and that between serotypes 1 and 14 suggested that the side chain constitutes one important antigenic determinant for serotypes 1, 1/2, and 2. In contrast, serotype 14 CPS specifically elicits an antibody response against its backbone. These results contribute to the understanding of the relationship between *S. suis* serotypes and provide the basis for improving diagnostic tools.

Experimental Procedures

Capsular Polysaccharide Isolation and Purification—*S. suis* serotype 1 strain 1178027, isolated from the meninges of a diseased pig in Canada,[4] and serotype 1/2 strain 2651, isolated from a diseased pig in Denmark (2), were used in this study. Bacterial growth, capsule extraction, and CPS purification were performed essentially as described previously (10). Gel filtration fractions giving a differential refractometer signal but no UV absorption at 280 and 254 nm were considered to be CPS. This was further confirmed by dot-blotting of all fractions with anti-*S. suis* serotype 1 or 2 serum (6).

[4] M. Gottschalk, unpublished data.

Quality Controls—Nucleic acids and proteins were quantified essentially as described previously (10).

Mild Acid Hydrolysis—To obtain desialylated polysaccharides for structural and serological studies, mild acid hydrolyses were performed essentially as described previously (10).

Physicochemical Characterization—Polysaccharides were characterized by size exclusion chromatography coupled with multiangle light scattering essentially as described previously (10).

Chemical and GC Analyses—Sugar analyses by methanolysis and hydrolysis, determination of absolute enantiomeric configuration, glycosidic linkage analysis, and GC or GC-MS analysis were performed essentially as described previously (10).

Enzyme-linked Lectin Assay to Detect the Presence of Sialic Acid—To verify the presence or absence of sialic acid in the purified native CPSs and the mild acid-hydrolyzed polysaccharides, an enzyme-linked lectin assay (ELLA) test was carried out with the *Sambucus nigra* agglutinin lectin (Vector Laboratories, Burlington, Canada), which specifically recognizes sialic acid as α-Neu5Ac-2,6-D-Gal*p*/Gal*p*NAc (12). Skimmed milk was used as a positive control. Group B *Streptococcus* type V CPS, which possesses an α-Neu5Ac-2,3-D-Gal*p* sequence, was purified as described previously (13) and used as a negative control. The assay was performed as described previously (13).

NMR Spectroscopy—Native CPSs and the 2-*O*-methyl-α-D-*N*-acetylneuraminic acid standard were exchanged in phosphate buffer, pD 8.0, in D_2O (99.9 atom % D), freeze-dried, and dissolved in D_2O (99.96 atom % D) to a final phosphate concentration of 33 mmol/liter. The mild acid-hydrolyzed polysaccharide and the neutral methyl glycoside standards were exchanged in D_2O (99.9 atom % D), freeze-dried, and dissolved in D_2O (99.96 atom % D). NMR spectra were acquired on polysaccharide samples at concentrations of ~1%. ^1H and ^{13}C chemical shifts δ in ppm were both referenced with internal deuterated 2,2-dimethyl-2-silapentane-5-sulfonate (DSS-d_6) at δ 0 as recommended by Wishart *et al.* (14).

NMR spectra were acquired at 11.75 T on a Bruker Avance 500 spectrometer equipped with a 5-mm triple-resonance TBI probe with ^1H, ^{13}C, and ^{109}Ag–^{31}P channels at 65 °C and at 16.45 T on a Bruker Avance 700 spectrometer with a 5-mm cryoprobe with ^1H and ^{13}C channels at 42, 56, or 70 °C using standard Bruker pulse sequences at the Regional Centre of NMR of the Department of Chemistry (University of Montreal). Conventional ^1H one-dimensional spectra were acquired with 30 or 90° pulses without or with water presaturation, respectively. The *z*-restored spin echo was used to acquire the ^1H-decoupled ^{13}C one-dimensional spectrum of straight baseline. The one-dimensional distortionless enhancement by polarization transfer (DEPT) spectrum was recorded with a reading pulse of 135° and the free precession period optimized for the 145-Hz one-bond coupling constant. The gradient-enhanced two-dimensional COSY experiment was performed in magnitude mode. The phase-sensitive two-dimensional total correlation spectroscopy (TOCSY) with Malcom Levitt's sequence (MLEV) was acquired with an effective spin lock time of 80 or 100 ms. The phase-sensitive two-dimensional rotating frame nuclear Overhauser effect spectroscopy (ROESY) using purge pulses before the relaxation delay, the phase-sensitive

two-dimensional ROESY with presaturation, and the phase-sensitive gradient-enhanced two-dimensional ROESY without TOCSY (T-ROESY) using echo-antiecho were acquired with a mixing time of 300 ms. The phase-sensitive gradient-enhanced two-dimensional heteronuclear single-quantum coherence (HSQC) using a *z*-filter and selection before t_1 and the phase-sensitive gradient-enhanced two-dimensional HSQC using echo-antiecho and adiabatic pulses for inversion and refocusing and Bloch-Siegert effects were optimized for 145 Hz. The phase-sensitive gradient-enhanced two-dimensional HSQC-TOCSY with MLEV using echo-antiecho was performed with a delay optimized for a 140-Hz coupling constant and a mixing time of 80 or 100 ms. The magnitude mode gradient-enhanced two-dimensional heteronuclear multiple-bond coherence (HMBC) using a low pass *J*-filter and the phase-sensitive gradient-enhanced two-dimensional HMBC using a 3-fold low pass *J*-filter were run without carbon decoupling with one-bond and long range delays optimized for 145 and 8 Hz, respectively. Spectra were processed off-line with SpinWorks (Kirk Marat, University of Manitoba). Zhu-Bax forward-backward linear prediction (15) with 16 coefficients was systematically applied to two-dimensional processing in the f_1 dimension.

Serological Analysis—Serotyping of reference strains by the coagglutination test, which is considered the "gold standard" in *S. suis* strain identification and typing, was performed at the International Reference Laboratory for *S. suis* Serotyping (University of Montreal). The reaction, which is done using formalin-fixed whole bacteria cultures with reference monospecific polyclonal rabbit sera against *S. suis* serotype 1, 1/2, 2, or 14, was performed as described previously (6). In addition, dot-blot analyses were performed as described previously by Calzas *et al.* (13). Ten microliters of purified native CPS or desialylated polysaccharide (each at 1 mg/ml in 50 mmol/liter NH_4HCO_3) for serotypes 1, 2, 1/2, and 14 were blotted on a PVDF Western blot membrane (Roche Diagnostics, Basel, Switzerland). The membrane was blocked for 1 h with a solution of TBS containing 2% casein, followed by 2 h of incubation with monospecific polyclonal rabbit sera (6). The membrane was washed, and anti-rabbit HRP-conjugated antibody (Jackson Immunoresearch, West Grove, PA) was added for 1 h. The membrane was washed three times with TBS and revealed with a 4-chloro-1-naphthol solution (Sigma-Aldrich, St. Louis, MO). Densitometric analysis of dot-blot scans was performed using ImageJ version 1.49 (16). Raw integration values were normalized using respective homologous signal values with native CPS.

Results

Capsular Polysaccharide Purification Yield and Quality Controls—From 6 liters of fermentation broth in different experiments, CPS yields after purification by gel filtration were 31–44 mg for serotype 1 and 72–75 mg for serotype 1/2. Nucleic acid analysis confirmed the absence of significant contamination, giving 0.4 and 0.2% DNA/RNA for serotypes 1 and 1/2, respectively. Similarly, no significant level of protein contamination was detected in the purified CPSs.

Mild Acid Hydrolysis and Physicochemical Characterization—Chemical modification of the native CPSs was performed by mild acid hydrolysis without complete depolymerization of the polysaccharide. This was demonstrated by physicochemical characterization by size exclusion chromatography coupled with multiangle light scattering. The native CPSs scattered light more intensely than the mild acid-hydrolyzed polysaccharides, because the mass of the polysaccharides was reduced by mild acid hydrolysis. For serotype 1, weight average molar weights ($\bar{M}_w$) of 7.410×10^5 g/mol and 1.567×10^5 g/mol were determined for the native and hydrolyzed polysaccharides, respectively. For serotype 1/2, $\bar{M}_w$ of 7.086×10^5 g/mol and 2.249×10^4 g/mol were determined for the native and hydrolyzed polysaccharides, respectively.

Chemical Analyses—Sugar composition of the CPSs determined after methanolysis and acetylation gave the ratios 0.0:1.6:1:0.6:0.9:1.1 and 1.1:1.4:1:0.4:1.0:0.5 for Rha/Gal/Glc/GalN/GlcN/Neu for serotypes 1 and 1/2, respectively, whereas the ratios 0.0:1:1.7:0.8:0.9 and 1.0:1:1.7:0.6:0.7 for Rha/Glc/Gal/GlcN/GalN were obtained following hydrolysis, reduction, and acetylation. The data are consistent with repeating units composed of 1 Glc, 2 Gal, 1 GlcN, 1 GalN, and 1 Neu for serotype 1 CPS and 1 Glc, 2 Gal, 1 Rha, 1 GlcN, 1 GalN, and 1 Neu for serotype 1/2 CPS.

In all cases, the absolute enantiomeric configurations were D for galactose, glucose, glucosamine, and galactosamine and L for rhamnose. The possibility of enzymatic hydrolysis with a specific sialidase has already confirmed the D-configuration for sialic acid for both CPSs (17).

Linkage positions were confirmed from GC retention times and MS fragmentation patterns of partially methylated alditol acetates (18). For the mild acid-hydrolyzed polysaccharide obtained from serotype 1 CPS, methylation analysis gave the ratio 1:0.5:0.5:0.9:1.0 for the derivatives 1,4,5-tri-*O*-acetyl-2,3,6-tri-*O*-methylglucitol, 1,3,5-tri-*O*-acetyl-2,4,6-tri-*O*-methylgalactitol, 1,3,5,6-tetra-*O*-acetyl-2,4-di-*O*-methylgalactitol, 2-acetamido-1,5-di-*O*-acetyl-2-deoxy-2,3,4,6-tetra-*O*-methylgalactitol, and 2-acetamido-1,4,5-tri-*O*-acetyl-2-deoxy-2,3,6-tri-*O*-methylglucitol, indicative of the linkage types 4-linked Glc, 3-linked Gal, 3,6-linked Gal, terminal GalN, and 4-linked GlcN, respectively. Derivatives 1,5-di-*O*-acetyl-2,3,4,6-tetra-*O*-methylgalactitol, 1,3,4,5-tetra-*O*-acetyl-6-deoxy-2-*O*-methylmannitol, 1,4,5-tri-*O*-acetyl-2,3,6-tri-*O*-methylglucitol, 1,3,4,5-tetra-*O*-acetyl-2,6-di-*O*-methylgalactitol, 2-acetamido-1,5-di-*O*-acetyl-2-deoxy-2,3,4,6-tetra-*O*-methylgalactitol, and 2-acetamido-1,4,5-tri-*O*-acetyl-2-deoxy-2,3,6-tri-*O*-methylglucitol, corresponding to the linkage types terminal Gal, 3,4-linked Rha, 4-linked Glc, 3,4-linked Gal, terminal GalN, and 4-linked GlcN, respectively, were detected for the mild acid-hydrolyzed polysaccharide obtained from serotype 1/2 CPS.

Lectin Binding—The *S. nigra* agglutinin lectin, which recognizes the Neu5Ac(α2–6)Gal/GalNAc sequence (12), showed binding to both native CPSs, indicating that the sialic acid residue is linked at position 6 of a galactose or an *N*-acetylgalactosamine residue (Fig. 1).

NMR Spectroscopy of Serotype 1—The one-dimensional ^{1}H NMR spectrum of serotype 1 CPS (Fig. 2*A*) displayed five ano-

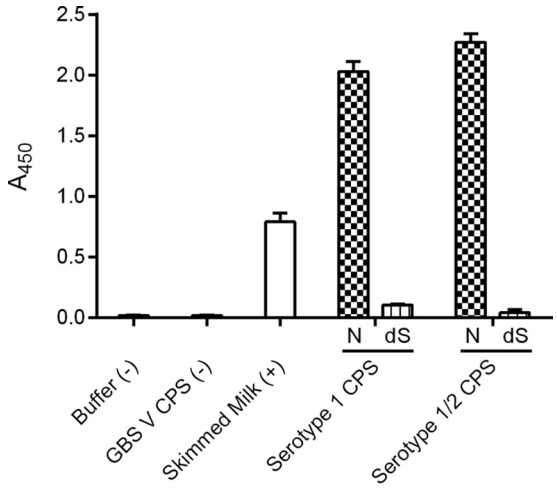

FIGURE 1. **ELLA of native and desialylated polysaccharides of *S. suis* serotypes 1 and 1/2 using *S. nigra* agglutinin.** *N*, native CPS preparations; *dS*, desialylated polysaccharide preparations per serotype. Data are shown as mean ± S.E. (*error bars*). ELLA experiments were performed at least twice. *GBS*, Group B *Streptococcus*.

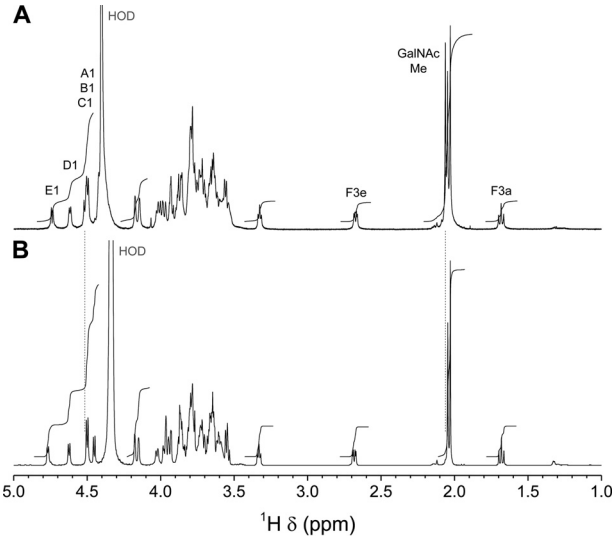

FIGURE 2. **700.3-MHz one-dimensional ^{1}H NMR spectra of *S. suis* CPSs in phosphate buffer, pD 8.0, in D_2O.** *A*, serotype 1, 33 mmol/liter, 70 °C. 32,768 complex data points were acquired with a digital resolution of 0.21 Hz/point and processed by exponential multiplication, zero filling, Fourier transform, phase correction, and fifth-order polynomial least-squares baseline correction. *B*, serotype 14, 80 mmol/liter, 77 °C. 16,384 complex data points were acquired with a digital resolution of 0.31 Hz/point and processed as above. *Vertical dotted lines* indicate major differences between the two spectra.

meric signals, three acetyl methyl signals, and two methylene signals characteristic of sialic acid at δ 2.68 and 1.68. The chemical shift of the latter axial H-3 is consistent with a 2,6-linkage to a galactopyranose ring (19). Residues were labeled A–E in order of increasing chemical shift of their anomeric protons. From the large coupling constants displayed by their anomeric signals (Fig. 2*A* and Table 1), these five residues have the β anomeric configuration. In the above reporter resonance regions, differences with serotype 14 CPS (Fig. 2*B*) were minor; one H-1 signal shifted to higher frequency, and one extra CH_3 signal (δ 2.06) from the *N*-acetylgalactosamine residue was present.

The ^{13}C NMR spectrum (supplemental Fig. S1*A*) displayed reporter resonance peaks: four carbonyl carbons (three acetyl; one carboxyl in position 1 of sialic acid), six anomeric carbons, three amino carbons, one methylene carbon at δ 42.86, and three acetyl methyl carbons. The DEPT-135 spectrum (supplemental Fig. S1*B*) showed that only three of five CH_2 signals were in an unshifted position, characteristic of hexoses in the pyranose form unsubstituted at position 6, whereas other methylene signals were shifted to higher frequencies (δ 66.06 and 71.47), confirming a linkage at position 6 for two sugar residues. In addition, the methylene signal at δ 65.56 was attributed to C-9 of sialic acid, and one quaternary carbon signal in the anomeric region (δ 103.00) corresponded to C-2 of sialic acid.

On the COSY spectrum (Fig. 3), spin systems could be followed up to H-2 for residues A, D, and E and H-3 for residues B and C. The width of the H-1–H-2 cross-peaks confirmed the β anomeric configuration for residues A–D. Spin systems were further extended with the TOCSY spectrum (supplemental Fig. S2). For certain residues (e.g. B and E), it was possible to follow the spin system from position 1 to positions 5 and 6, because coupling constants were large and magnetization propagated easily, indicating a *β-gluco* configuration. In other cases, as for residues A and D, propagation from the anomeric protons stopped at position 4, which is typical for the *β-galacto* configuration. Starting from the protons in position 3 of sialic acid, the TOCSY spectrum (supplemental Fig. S2) displayed correlations to protons in positions 4–6. Some of the remaining protons could be assigned from the ROESY spectrum (supplemental Fig. S3), which clearly displayed correlations between H-1 and H-5 for residues A–E. With the above additional information from TOCSY and ROESY, further analysis of the COSY spectrum gave nearly complete assignments for most spin systems. In the end, only a few ambiguities remained as to the assignment of protons in position 6 for residues A, B, and D.

The ^{13}C chemical shift of E2 found on the HSQC spectrum (Fig. 4) at lower frequency (δ 57.66) indicates that residue E corresponds to *N*-acetylglucosamine, leaving residue B as glucose. Similarly, the ^{13}C chemical shift of C2 (δ 55.24) indicates that residue C corresponds to *N*-acetylgalactosamine, leaving residues A and D as galactose. Carbons of the sialic acid residue F were assigned by comparison with the methyl glycoside of *N*-acetylneuraminic acid and with corresponding signals in the *S. suis* serotype 14 and 2 CPSs (10, 11). On the HSQC-TOCSY spectrum (supplemental Fig. S4), protons in position 5 previously found on the ROESY spectrum allowed the assignment of protons in position 6, based on long range correlations at their C-5 chemical shifts, from which corresponding C-6 resonances could be assigned.

When compared with corresponding methyl glycosides, ^{13}C NMR α-glycosidation shifts of 2.30–10.63 ppm were observed for carbons A3, B4, C6, D3, D6, and E4. These results confirm the linkage analysis data for all sugars: 3-linked Gal (A), 4-linked Glc (B), 6-linked GalNAc (C) (terminal GalNAc in the desialylated polysaccharide), 3,6-linked Gal (D), 4-linked GlcNAc (E), and terminal Neu5Ac (F). On the ROESY spectrum (supplemental Fig. S3), a few interresi-

TABLE 1

NMR chemical shifts of *S. suis* serotype 1 native CPS

Shown are chemical shifts ($^1H/^{13}C$) in 33 mmol/liter phosphate buffer, pD 8.0, in D_2O in ppm referenced to internal DSS. ^1H chemical shifts were obtained at 70 °C from the one-dimensional spectrum, at 65 °C from the COSY or TOCSY spectrum, or at 70 °C from the HSQC spectrum. ^{13}C chemical shifts were obtained at 70 °C from the one-dimensional spectrum.

Residue		1	2	3		4	5	6		7	8	9		Me	CO
A	→3)-β-D-Gal-(1→	4.49 (7.8)[a]	3.71	3.80		4.17	3.73	3.77							
		105.30[b]	72.87[b]	84.81		71.06	77.65	63.68							
B	→4)-β-D-Glc-(1→	4.49 (7.8)	3.33	3.63		3.64	3.58	3.97	3.80						
		105.29[b]	75.54	77.19		81.28	77.51	63.00							
C	→6)-β-D-GalNAc-(1→	4.52 (8.4)	3.93	3.74		3.93	3.79	4.00	3.61					2.06	
		104.77	55.24	73.43		70.28	76.42	66.06						24.97	177.30
D	→3,6)-β-D-Gal-(1→	4.62 (7.5)	3.66	3.73		4.13	3.85	4.02	3.85						
		106.83	72.88[b]	84.49		70.97	75.85	71.47							
E	→4)-β-D-GlcNAc-(1→	4.74 (7.5)	3.78	3.78		3.55	3.54	3.82	3.64					2.05	
		105.14	57.66	75.11		83.54	76.89	63.03						25.08	177.49
F	α-D-Neu5Ac-(2→			2.68	1.68	3.68	3.77	3.71		3.56	3.88	3.87	3.65	2.03	
		175.97	103.00	42.86		70.87	54.74	75.30		71.31	74.46	65.56		24.77	177.66

[a] Coupling constants ($J_{H\text{-}1\text{–}H\text{-}2}$) in parentheses.
[b] Tentative assignments.

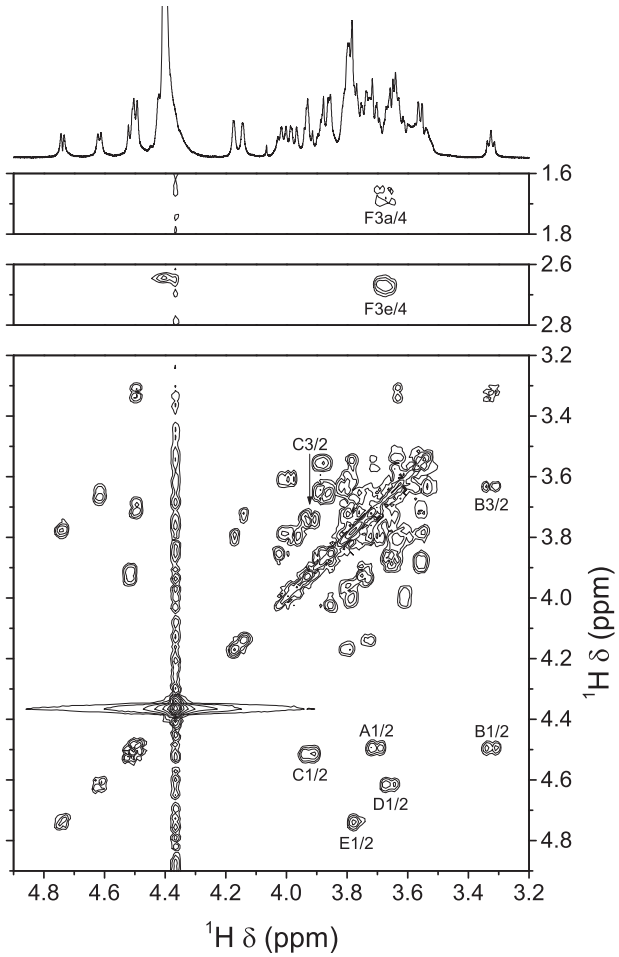

FIGURE 3. **Portions of the 500.1-MHz gradient-enhanced two-dimensional COSY spectrum of *S. suis* serotype 1 CPS in 33 mmol/liter phosphate buffer, pD 8.0, in D_2O at 65 °C.** 512 increments of 1024 complex data points were acquired in magnitude mode with a digital resolution of 4.9 Hz/point in the t_2 dimension and 9.8 Hz/point in the t_1 dimension. The t_2 dimension was processed by multiplication with an unshifted sine bell window function and Fourier transform, and the t_1 dimension was processed by Zhu-Bax linear prediction to 1024 points, multiplication with an unshifted sine bell window function, Fourier transform, and magnitude calculation. The f_2 trace corresponds to the one-dimensional spectrum (see Fig. 2*A*).

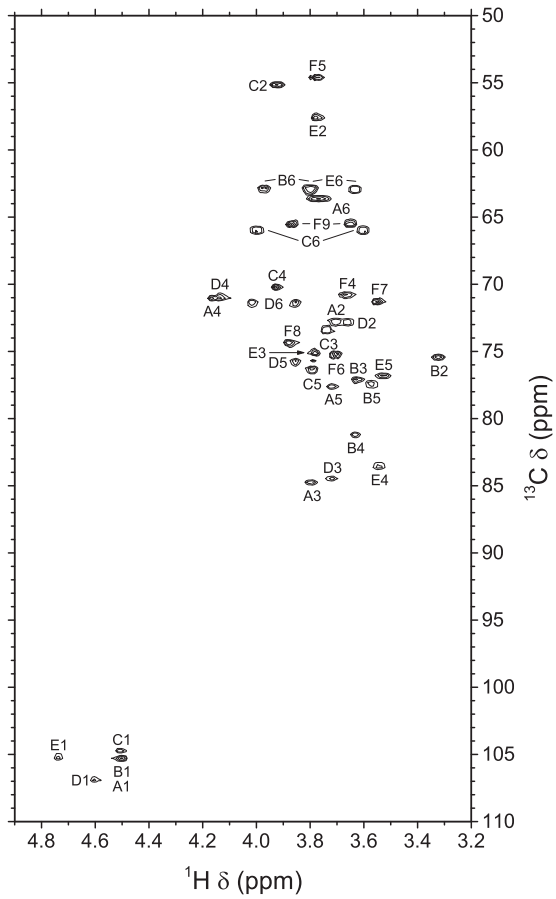

FIGURE 4. **Portion of the 700.3-MHz gradient-enhanced two-dimensional HSQC spectrum of *S. suis* serotype 1 CPS in 33 mmol/liter phosphate buffer, pD 8.0, in D_2O at 70 °C.** 2 × 256 increments of 819 complex data points were acquired in the States-time-proportional phase increment mode with a digital resolution of 6.8 Hz/point in the t_2 dimension and 96.3 Hz/point in the t_1 dimension. The t_2 dimension was processed by multiplication with a $\pi/2$ shifted sine bell window function, zero filling, Fourier transform, and phase correction, and the t_1 dimension was processed by Zhu-Bax linear prediction to 512 points, multiplication with a $\pi/2$ shifted sine bell window function, Fourier transform, and phase correction. Only positive contours are shown.

due correlations could readily be identified: B4/A1, D5/B1, D6/B1, E4/C1, E5/C1, A3/D1, D2/E1, and D3/E1. However, these through-space correlations do not necessarily correspond to linkage positions. In contrast, interresidue correlations found on the HMBC spectrum (supplemental Fig. S5), both from anomeric carbons (A1/B4, B1/D6, C1/E4, D1/A3, E1/D3, and F2/C6) and to anomeric protons (B4/A1, D6/B1,

F C E

α-D-Neu*p*5Ac-(2→6)-β-D-Gal*p*NAc-(1→4)-β-D-Glc*p*NAc

1

↓

3

[6)-β-D-Gal*p*-(1→3)-β-D-Gal*p*-(1→4)-β-D-Glc*p*-(1→]$_n$

D A B

SCHEME 1. **Structure of *S. suis* serotype 1 CPS with residue labels.**

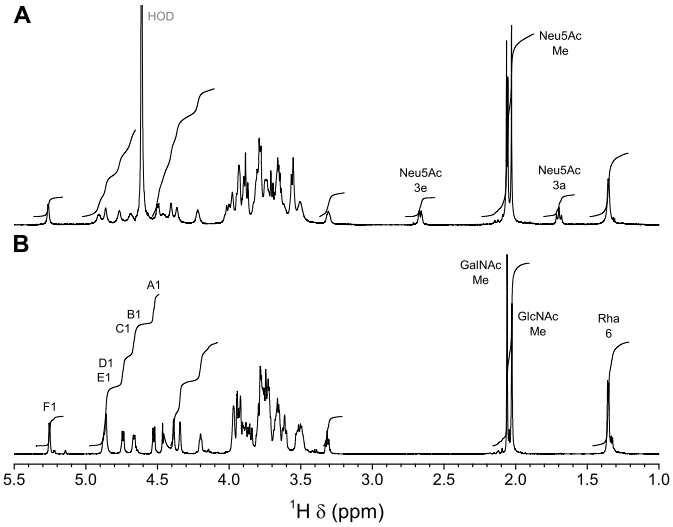

FIGURE 5. **700.3-MHz one-dimensional ^{1}H NMR spectra of *S. suis* serotype 1/2 polysaccharides.** *A*, native CPS in 33 mmol/liter phosphate buffer, pD 8.0, in D_2O at 42 °C. 40,960 complex data points were acquired with a digital resolution of 0.18 Hz/point and processed as for Fig. 2*A*. *B*, desialylated polysaccharide in D_2O at 56 °C. 40,960 complex data points were acquired with presaturation with a digital resolution of 0.17 Hz/point and processed as above.

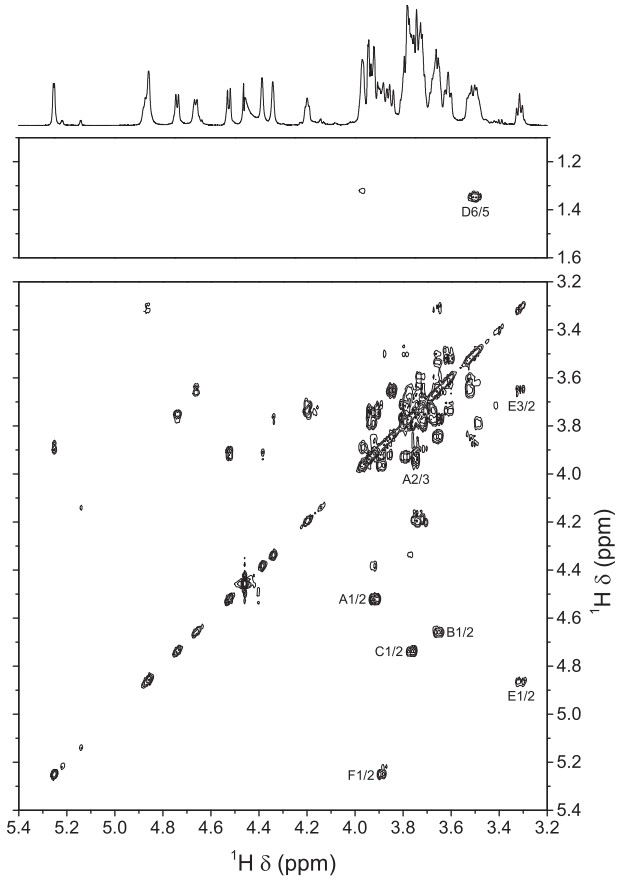

FIGURE 6. **Portions of the 700.3-MHz gradient-enhanced two-dimensional COSY spectrum of *S. suis* serotype 1/2 desialylated polysaccharide in D_2O at 56 °C.** 512 increments of 2048 complex data points were acquired in magnitude mode with a digital resolution of 3.4 Hz/point in the t_2 dimension and 13.7 Hz/point in the t_1 dimension. Processing was as for Fig. 3. The f_2 trace corresponds to the one-dimensional spectrum (see Fig. 5*B*).

E4/C1, A3/D1, and D3/E1), confirmed the true linkage positions for all residues (Scheme 1).

Finally, the structure was built in the program CASPER (20). Root mean square deviations between experimental and calculated ^{1}H and ^{13}C chemical shifts were 0.05 and 0.26 ppm, respectively.

NMR Spectroscopy of Serotype 1/2—All characteristics of the ^{1}H NMR spectra of serotype 1/2 polysaccharides before and after mild acid hydrolysis (Fig. 5) were identical to those described for the corresponding serotype 2 polysaccharides (11), and similarly, the structure was first determined using the partially hydrolyzed desialylated polysaccharide.

The one-dimensional ^{13}C spectrum (supplemental Fig. S6*A*) displayed reporter resonance peaks: two acetyl carbonyl carbons; six anomeric carbons; two amino carbons (C-2) of *N*-acetylhexosamines; and two methyl carbons corresponding to acetyl of *N*-acetylhexosamines and one corresponding to position 6 of rhamnose. Identical information regarding substitution on position 6 and the pyranose ring form was obtained from the DEPT-135 spectrum (supplemental Fig. S6*B*) as for the serotype 2 desialylated polysaccharide (11).

Analysis of the COSY (Fig. 6) and TOCSY (supplemental Fig. S7) spectra gave essentially the same information about anomeric configuration and identity of residues as for the serotype 2 desialylated polysaccharide (11). As for serotype 1 CPS, the ROESY spectrum (supplemental Fig. S8) displayed correlations between H-1 and H-5 for all residues. After full assignment of the proton spectrum (Table 2), the only missing chemical shifts at this stage were those of position 6 of residues A and E.

From the ^{13}C chemical shifts of A2 and C2 found on the HSQC spectrum (Fig. 7) at lower frequency (δ 55.33 and 57.99), residues A and C were assigned to *N*-acetylgalactosamine and *N*-acetylglucosamine, respectively, leaving residues B and E as galactose and glucose, respectively. Protons in position 6 of residue E were found on the HSQC-TOCSY spectrum (supplemental Fig. S9), and thus the last carbon peak could be assigned to A6 by default.

When compared with corresponding methyl glycosides, α-glycosidation shifts of 2.4–9.5 ppm were observed for carbons B3, B4, C4, D3, D4, and E4. These results confirmed the linkage analysis data for all sugars: terminal Gal (F), 3,4-linked Rha (D), 4-linked Glc (E), 3,4-linked Gal (B), terminal GalNAc (A), and 4-linked GlcNAc (C). On the ROESY spectrum (supplemental Fig. S8), a few interresidue correlations could readily be identified: A1/C2–6, B1/D3–4, C1/B3, E1/B4, and F1/D2. These through-space correlations do not necessarily correspond to linkage positions, in part because TOCSY peaks were not suppressed. In contrast, on the HMBC spectrum (supplemental Fig. S10), C4, D4, B3, E4, B4, and D3 were confirmed as the true linkage positions for residues A–F, respectively. The

TABLE 2

NMR chemical shifts of *S. suis* serotype 1/2 desialylated polysaccharide

Shown are chemical shifts ($^1H/^{13}C$) in D_2O in ppm referenced to internal DSS. ^1H chemical shifts were obtained at 56 °C from the one-dimensional, COSY, TOCSY, or HSQC spectrum. ^{13}C chemical shifts were obtained at 56 °C from the one-dimensional or HSQC spectrum.

Residue		1	2	3	4	5	6		Me	CO
A	β-D-GalNAc-(1→	4.53 (8.3)[a]	3.92	3.75	3.94	3.72	3.78		2.06	
		104.47	55.33	73.43	70.40	78.01	63.64		24.96	177.39
B	→3,4)-β-D-Gal-(1→	4.66 (7.3)	3.65	3.77	4.35	3.68	3.78	3.76		
		105.67	73.2[b]	85.13	77.8[b]	76.9[b]	63.32			
C	→4)-β-D-GlcNAc-(1→	4.74 (7.8)	3.76	3.73	3.61	3.52	3.85	3.66	2.03	
		105.55	57.99	75.19	82.16	77.22	63.07		25.10	177.35
D	→3,4)-β-L-Rha-(1→	4.86	4.39	3.93	3.87	3.50	1.35			
		103.1[b]	68.40	77.99	78.6[b]	73.84	19.94			
E	→4)-β-D-Glc-(1→	4.87	3.32	3.66	3.61	3.49	3.93	3.79		
		104.7[b]	76.3[b]	78.4[b]	80.0[b]	77.15	63.81			
F	α-D-Gal-(1→	5.25 (3.4)	3.89	3.97	3.97	4.20	3.73			
		95.80	70.95	72.24[c]	72.14[c]	73.79	63.91			

[a] Coupling constants ($J_{H\text{-}1,H\text{-}2}$) in parentheses.
[b] Obtained from the HSQC spectrum.
[c] Tentative assignments.

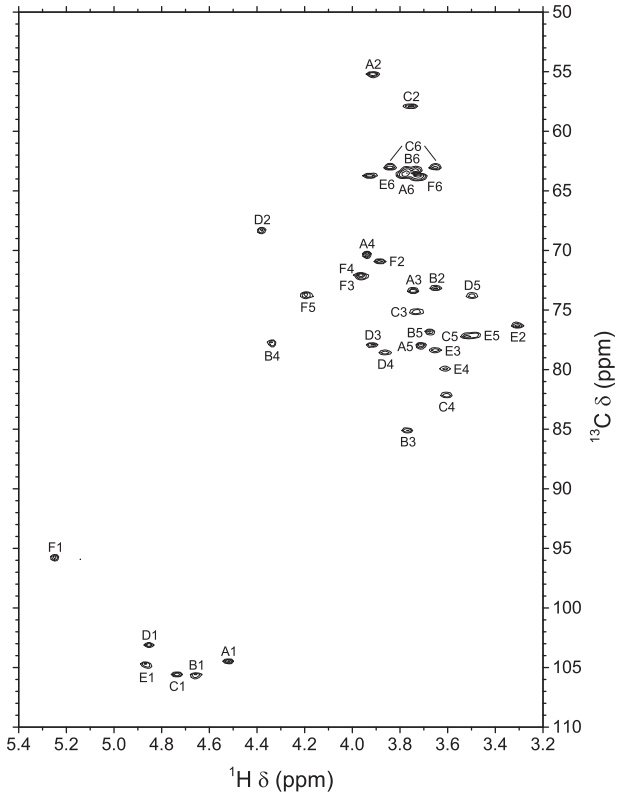

FIGURE 7. **Portion of the 700.3-MHz gradient-enhanced two-dimensional HSQC spectrum of *S. suis* serotype 1/2 desialylated polysaccharide in D_2O at 56 °C.** 2 × 200 increments of 700 complex data points were acquired in the echo-antiecho mode with a digital resolution of 10.0 Hz/point in the t_2 dimension and 101.2 Hz/point in the t_1 dimension. The t_2 dimension was processed by multiplication with a $\pi/2$ shifted sine bell window function, zero filling, Fourier transform, and phase correction, and the t_1 dimension was processed by Zhu-Bax linear prediction to 400 points, multiplication with a $\pi/2$ shifted sine bell window function, zero filling, Fourier transform, and phase correction. Only positive contours are shown.

structure shown in Scheme 2 is consistent with the connectivity data obtained from the HMBC and ROESY spectra.

By analogy with serotype 2 CPS (11), we postulated that sialic acid was linked to position 6 of the terminal *N*-acetylgalactosamine residue (A), giving the structure shown in Scheme 3 for serotype 1/2 native CPS.

This hypothesis was confirmed by analyzing the differences in the NMR spectra of the two polysaccharides (Tables 2 and 3).

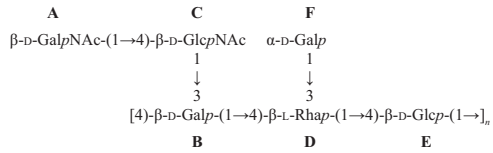

SCHEME 2. **Structure of *S. suis* serotype 1/2 desialylated polysaccharide with residue labels.**

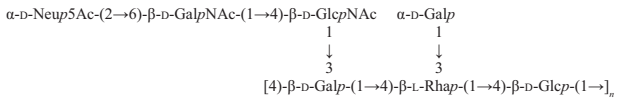

SCHEME 3. **Structure of *S. suis* serotype 1/2 CPS.**

On the DEPT-135 spectrum of the native CPS (not shown), additional reporter resonance signals at approximately δ 54.7, 42.9, and 24.8, corresponding to C-5, C-3, and acetyl methyl of *N*-acetylneuraminic acid, respectively, were present. In addition, methylene signals at approximately δ 66.1 and 65.5 were attributed to C-6 of a substituted hexosamine residue and to C-9 of sialic acid, respectively. The following quaternary carbons were found on the ^{13}C spectrum (not shown): four signals in the carbonyl region belonging to three acetyls and one carboxyl at position 1 of sialic acid as well as one signal in the anomeric region (δ 102.91) corresponding to C-2 of sialic acid. The two-dimensional TOCSY spectrum (not shown) gave correlation information identical to that of serotype 2 CPS (11). The ^{13}C NMR spectrum of the native CPS was assigned from HSQC (supplemental Fig. S11) essentially by comparison with that of the desialylated polysaccharide for residues A–F, whereas carbons of the sialic acid residue G were assigned as for serotype 1 CPS. Carbons A6, B3, C4, D3, D4, and E4 displayed α-glycosidation shifts of 2.4–11.0 ppm when compared with the corresponding methyl glycosides; however, carbon B4 was not observed, probably due to restricted motion of this branching residue. As for serotype 2 CPS (11), the only ^{13}C chemical shifts to move appreciably (>1 S.D. in either direction) upon desialylation were those of carbons A5 (+1.58 ppm), A6 (−2.48 ppm), and C4 (−1.71 ppm). The following interresidue correlations were unambiguously present on the ROESY spectrum (not shown): A1/C4–5 and F1/D2. Finally, the HMBC (not shown) allowed assignment of the carbonyl carbons.

TABLE 3

NMR chemical shifts of *S. suis* serotype 1/2 native CPS

Shown are chemical shifts ($^1H/^{13}C$) in 33 mmol/liter phosphate buffer, pD 8.0, in D_2O in ppm referenced to internal DSS. ^1H chemical shifts were obtained at 42 °C from the one-dimensional, COSY, TOCSY, or HSQC spectrum. ^{13}C chemical shifts were obtained at 42 °C from the one-dimensional spectrum.

Residue		1	2	3		4	5	6		7	8	9		Me	CO
A	→6)-β-D-GalNAc-(1→	4.50 (8.1)[a]	3.94	3.74		3.93	3.80	4.02	3.56					2.06	
		104.95	55.18	73.40		70.20	76.44	66.12						24.98	177.41
B	→3,4)-β-D-Gal-(1→	4.69	3.66	3.79		4.36	3.70	3.77	3.74						
		105.72	73.10	85.22		ND[b]	76.92	63.33							
C	→4)-β-D-GlcNAc-(1→	4.77	3.78	3.78		3.55	3.55	3.82	3.64					2.05	
		105.55	57.73	75.31		83.87	76.92	63.18						26.27	177.41
D	→3,4)-β-L-Rha-(1→	4.86	4.41	3.93		3.87	3.51	1.35							
		103.29	68.28	77.84		78.43	73.81	19.95							
E	→4)-β-D-Glc-(1→	4.91	3.31	3.67		3.62	3.50	3.94	3.81						
		104.60	76.25	78.43		80.12	77.15	63.74							
F	α-D-Gal-(1→	5.26	3.89	3.99		3.98	4.22	3.73							
		95.60	70.94	72.20[c]		72.15[c]	73.81	63.97							
G	α-D-Neu5Ac-(2→			2.67	1.70	3.66	3.79	3.70		3.56	3.90	3.88	3.64	2.03	
		176.13	102.91	42.87		70.88	54.70	75.31		71.23	74.45	65.48		24.79	177.71

[a] Coupling constant ($J_{H\text{-}1\text{–}H\text{-}2}$) in parentheses.
[b] Not determined.
[c] Tentative assignments.

Serological Characteristics—Table 4 presents the cross-reactions obtained between serotypes 1, 1/2, 2, and 14 of *S. suis* using the internationally recognized coagglutination test (performed at the International Reference Laboratory for *S. suis* Serotyping). Serotype 1 strongly reacts with anti-serotype 14 serum, although a serotype 14 strain remains negative/weak with the anti-serotype 1 serum (Table 4). Serotype 1/2 is defined as being positive for both anti-serotype 1 and 2 sera. Although never used as a reagent for serotyping, an anti-serotype 1/2 serum was produced in rabbits and showed positive reactions with serotype 1 and 1/2 strains but resulted in a negative reaction with the serotype 2 reference strain (Table 4).

To better understand these serological cross-reactions and the possible structural elements involved, dot-blot experiments were performed using native and desialylated polysaccharides (Fig. 8). Complete desialylation of the mild acid-hydrolyzed CPSs was confirmed by NMR (data not shown) and by ELLA (Fig. 1) for serotypes 1 and 1/2. Complete desialylation of serotype 2 and 14 CPSs has been previously and routinely performed (10, 11, 13, 21).

Anti-serotype 1 serum showed a strong reaction with serotype 1 and a weaker response with serotype 14 for both native and desialylated polysaccharides (Fig. 8, *A* and *E*). However, native and desialylated polysaccharides of serotypes 1 and 14 were similarly recognized by anti-serotype 14 serum (Fig. 8, *B* and *F*). The weaker recognition of serotype 14 CPS by anti-serotype 1 serum suggests that the *N*-acetylgalactosamine moiety bearing the sialic acid is part of a major immunogenic sequence for serotype 1 CPS. Thus, substitution of the *N*-acetylgalactosamine residue by a galactose in serotype 14 CPS might result in a lower affinity of an anti-serotype 1 serum for serotype 14, whereas the absence of sialic acid does not show a substantial effect (Fig. 9*A*). On the other hand, this part of the CPS structure does not seem to play a role in the recognition of serotype 1 CPS by anti-serotype 14 serum. In fact, for serotype 14, the major immunogenic part might reside in the polysaccharide backbone sequence (Fig. 9*A*), which would explain the equal recognition of serotypes 1 and 14 by anti-serotype 14 serum and the non-recognition of serotype 1/2 CPS (Fig. 8, *B* and *F*). For both anti-serotype 1 and 14 sera, no detection of serotype 2 CPS occurred, illustrating important structural/conformational (and, in consequence, antigenic) differences between serotype 1 and 14 dominant epitopes and those of serotype 2. In agreement with these data, anti-serotype 2 serum did not recognize serotype 1 and 14 CPSs (Fig. 8, *C* and *G*).

Another important cross-reaction is that between serotype 1/2 CPS and anti-serotype 1 and 2 sera. Dot-blots showed that only serotype 1/2 native CPS was recognized by anti-serotype 1 serum (Fig. 8, *A* and *E*). Indeed, the absence of sialic acid in serotype 1/2 CPS abolished this cross-reaction. Similarly, the removal of sialic acid also almost completely abolished recognition of serotype 1/2 CPS by its homologous antiserum (Fig. 8, *D* and *H*). Inversely, serotype 1 native CPS was strongly recognized by anti-serotype 1/2 serum, and the absence of sialic acid in serotype 1 desialylated polysaccharide considerably reduced this cross-reaction (Fig. 8, *D* and *H*). The only common structure between these two serotypes is the Neu5Ac-(α2,6)-GalNAc-(β1,4)-GlcNAc side chain (Fig. 9*B*). However, compared with serotype 1, the presence of sialic acid in serotype 1/2 seems to play a major role in the immunogenic and cross-reactive properties of this serotype.

Similarly, only serotype 1/2 native CPS was significantly recognized by anti-serotype 2 serum (Fig. 8, *C* and *G*). This cross-reaction was, however, weaker than that observed when using anti-serotype 1 serum (Fig. 8, *A* and *E*). In addition, serotype 1/2 antiserum was unable to recognize either serotype 2 native CPS or desialylated polysaccharide (Fig. 8, *D* and *H*). This result was in agreement with that obtained with the coagglutination test using formalin-fixed whole *S. suis* serotype 2 (strain S735) culture as antigen (Table 4). The substitution of the *N*-acetylgalactosamine residue by a galactose in serotype 2 CPS side chain (Neu5Ac-(α2,6)-Gal-(β1,4)-GlcNAc) might explain the lower affinity of an anti-serotype 2 serum for serotype 1/2 and the absence of recognition of an anti-serotype 1/2 serum for serotype 2 CPS (Fig. 9*B*).

Finally, recognition by homologous anti-serotype 2 serum showed a stronger reaction with serotype 2 native CPS than with serotype 2 desialylated polysaccharide (Fig. 8, *C* and *G*), indicating that sialic acid is in fact part of one of the serotype 2

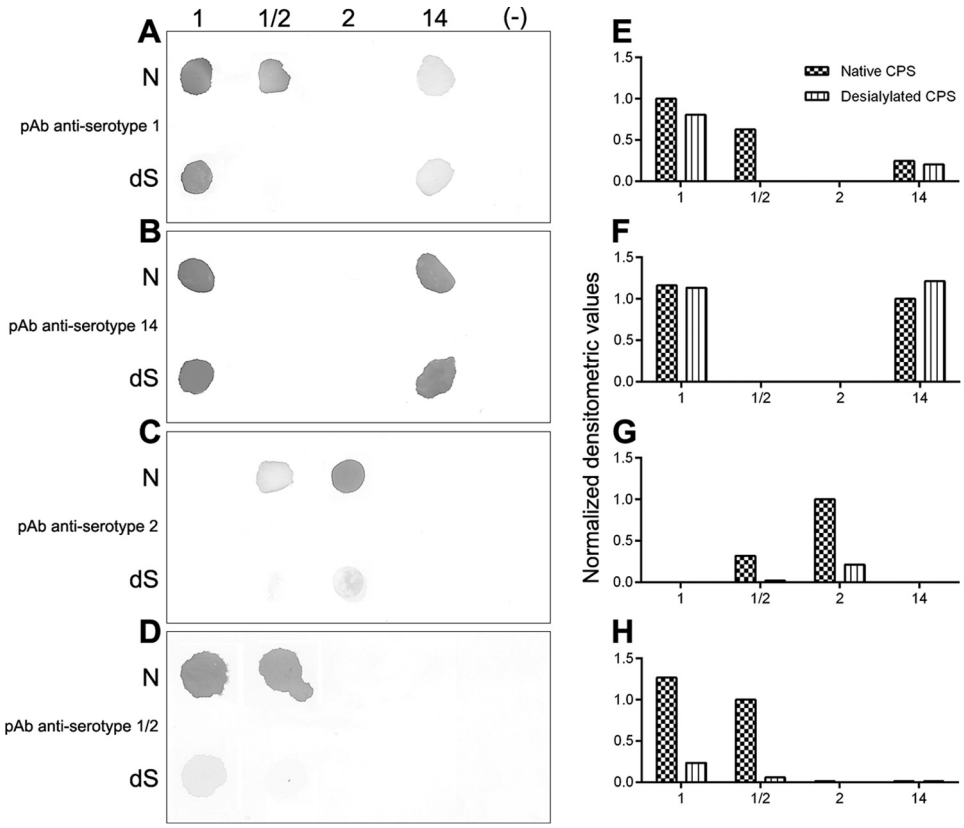

FIGURE 8. **Serological cross-reactions.** Dot-blot analyses with 10 μl each of native (*N*) CPS and desialylated (*dS*) polysaccharide preparations from serotypes 1, 1/2, 2, and 14 of *S. suis* using different rabbit polyclonal sera (*pAb*): anti-serotype 1 serum (*A*), anti-serotype 14 serum (*B*), anti-serotype 2 serum (*C*), or anti-serotype 1/2 serum (*D*). Negative control (−) is 50 mmol/liter NH_4HCO_3, which was used to dissolve all CPS preparations at 1 mg/ml. Normalized integration values obtained by densitometry analysis were calculated for each dot-blot: anti-serotype 1 serum (*E*), anti-serotype 14 serum (*F*), anti-serotype 2 serum (*G*), and anti-serotype 1/2 serum (*H*).

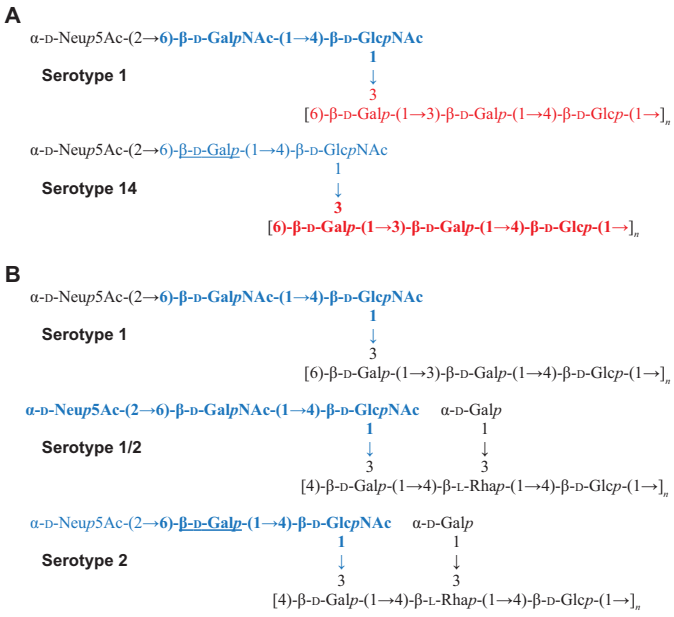

FIGURE 9. **Proposed structural elements recognized by type-specific antisera implicated in the serological cross-reactions between serotypes 1 and 14 (*A*) and between serotype 1/2 and serotypes 1 and 2 (*B*).** *Colored* elements represent those sequences probably involved in cross-reactions. *Red*, recognized structures from the backbone sequence; *blue*, structures from the side chains. *Boldface*, structures yielding the dominant antibody population. An *underline* is used to illustrate structural elements for which the cross-reaction is weaker.

immunogenic sequences. Altogether, these data indicate that the side chain (and, more particularly, the terminal sialic acid) constitutes one important immunogenic structure for serotype 1/2 and 2 CPSs. The side chain is also an important serological part of serotype 1 CPS structure, yet sialic acid seems to play a limited role. On the other hand, the side chain does not seem to be part of a major immunogenic reaction for serotype 14 CPS (Fig. 9, *A* and *B*).

Discussion

The CPS is the major virulence factor for several encapsulated pathogens, and it has been proven to be also the case for *S. suis*, at least for serotypes 2 and 14 (22–24). In addition, the CPS is the antigen at the origin of *S. suis* classification into serotypes. Due to the importance of the CPS to bacterial pathogenesis, the analysis of the CPS structure is an essential step not only to understand its role in virulence but also to dissect the serological relations between important serotypes.

The presence of a terminal sialic acid in the side chain is a common feature of all described serotypes of Group B *Streptococcus*, a human pathogen known to induce septicemia and meningitis, two pathologies also observed in cases of *S. suis* infection. For Group B *Streptococcus*, it has been proposed that sialic acid plays important modulatory roles in bacterial interactions with host cells and in the regulation of complement activation (25). Similarly to Group B *Streptococcus*, it has been suggested, based on chemical, genetic, and/or lectin binding

TABLE 4
Serological cross-reactions of *S. suis* when serotyping by the coagglutination method

Serotype (strain)	PBS[a]	Reference antiserum			
		Type 1	Type 1/2	Type 2	Type 14
Serotype 1 (1178027)	−	+++	+++	−	+++
Serotype 1/2 (2651)	−	++	+++	++	−
Serotype 2 (S735)	−	−	−	+++	−
Serotype 14 (DAN13730)	−	+/−	−	−	+++

[a] PBS was used as a negative control to ensure that formalin-fixed bacteria were not autoagglutinating.

analyses, that *S. suis* serotypes 1, 1/2, 2, 6, 13, 14, 15, 16, and 27 might also contain sialic acid in their CPSs (8, 9, 17, 26). The presence of this sugar was recently confirmed by CPS structural analyses in *S. suis* serotypes 2 and 14 (10, 11) and, in the present study, for serotypes 1 and 1/2. Interestingly, sialic acid forms an α-2,6-linkage with the adjacent sugar in *S. suis versus* an α-2,3-linkage in Group B *Streptococcus* (10, 11, 27, 28). However, the role of sialic acid in *S. suis* interactions with host cells or in modulation of the host immune system has been poorly characterized. It has been suggested that the sialic acid moiety of the *S. suis* serotype 2 CPS would be, at least in part, responsible for bacterial recognition by macrophages (29). More recently, it has been demonstrated that capsular sialic acid of *S. suis* serotype 2 binds to swine influenza virus and enhances bacterial interactions with virus-infected tracheal epithelial cells (30, 31). Thus, sialic acid might regulate host-pathogen interactions, yet its actual role in *S. suis* virulence remains to be elucidated.

For both serotype 1 and 1/2 CPSs, ^{1}H and ^{13}C NMR data are consistent with *N*-acetylgalactosamine replacing galactose as the sugar bearing the sialic acid residue, when compared with serotype 14 and 2 CPSs, respectively. Indeed, ^{13}C chemical shift differences between *N*-acetylgalactosamine and galactose residues in serotype 1 and 1/2 CPSs compared with serotype 14 and 2 CPSs are comparable with those between the corresponding methyl glycosides, methyl 2-acetamido-2-deoxy-β-D-galactopyranoside and methyl β-D-galactopyranoside (supplemental Table S1). The impact of this modification in the interactions of different *S. suis* serotypes (1 and 1/2 *versus* 2 and 14) with host cells or the immune system warrants further studies. In addition, higher yields of CPS were obtained for serotypes 1 and 1/2 compared with serotypes 2 and 14 (10, 11). Chain lengths (as represented by the $\bar{M}_w$ measured by size exclusion chromatography coupled with multiangle light scattering) for serotype 1 and 1/2 CPSs are both higher than those previously reported for serotypes 2 and 14 (10, 11), which might account for these differences in yields.

Another observed difference is that serotype 1 and 1/2 CPSs behave differently upon mild acid hydrolysis. Indeed, the reduction in mass is much more important for serotype 1/2 CPS than for serotype 1 CPS. This behavior was reported previously for serotype 2 CPS when compared with serotype 14 CPS (10). These observations support the hypothesis that the sugar residue rhamnose in the backbone of serotype 2 and 1/2 CPSs may be responsible for this behavior, because its linkages are more labile than those of the hexoses glucose and galactose (32).

Precise CPS structure analyses allowed for the first time a tentative explanation of the serological characteristics of *S. suis* serotypes 1, 1/2, 2, and 14. The structure of serotype 1 CPS was found to be sufficiently similar to that of serotype 14 CPS to explain its cross-reactivity with anti-serotype 14 serum and *vice versa*. Nevertheless, recognition of serotype 14 by anti-serotype 1 serum is weaker than homologous recognition, indicating that substitution of the *N*-acetylgalactosamine residue by a galactose in serotype 14 CPS side chain (Fig. 9*A*, *underlined*) affects optimal recognition by anti-serotype 1 serum. These results suggest that the main population of antibodies generated by serotype 1 CPS is directed against the side chain (Fig. 9*A*, *blue*). However, terminal sialic acid seems to be dispensable for antibody recognition in serotype 1 and for the cross-reaction with serotype 14. Although the side chain seems to harbor the major/dominant immunogenic part of serotype 1 CPS, we cannot rule out the production of antibodies against its backbone structure. This second, minor population of antibodies in the anti-serotype 1 serum can also cross-react to a certain extent with the backbone structure of serotype 14 CPS, being identical to that of serotype 1 CPS (Fig. 9*A*, *red*). On the other hand, the backbone part seems to be dominant in serotype 14 CPS, as suggested by equal intensity of homologous (serotype 14) and heterologous (serotype 1) recognition by the anti-serotype 14 serum. Our hypothesis that the backbone epitope is dominant in serotype 14 CPS is further supported by the lack of recognition of serotype 1/2 CPS, which has a side chain identical to that of serotype 1 CPS but a different backbone structure (Fig. 9*B*). Finally, despite the two CPSs having identical side chains, anti-serotype 14 serum does not react against serotype 2 CPS, further indicating that serotype 14 CPS specifically elicits antibody response against its backbone (Fig. 9).

Another so far unexplained cross-reaction is that of serotype 1/2 CPS with anti-serotype 2 and 1 sera. Our present study provided for the first time some insight into these cross-reactions. The side chain of serotype 1/2 CPS seems to be the target of cross-reactive antibodies present in anti-serotype 1 serum. This can be explained by identical structures of these two serotype CPS side chains (Fig. 9*B*). However, sialic acid seems to play an important role in serotype 1/2 CPS immunological recognition because its removal abolishes recognition not only by the homologous serum but also by anti-serotype 1 and anti-serotype 2 sera. The latter further suggests that the identical backbone structure between serotype 1/2 and 2 CPSs is, surprisingly, not essentially involved in the cross-reaction between these two serotypes. Investigation of anti-serotype 1/2 serum affinities supports previous conclusions. The main population of antibodies generated by serotype 1/2 CPS seems to be directed against its sialic acid-containing side chain, which explains a weaker cross-reaction with serotype 1 desialylated polysaccharide than that with serotype 1 native CPS.

The structural/conformational characteristics of serotype 2 CPS epitopes seem to be complex and remain hypothetical. For

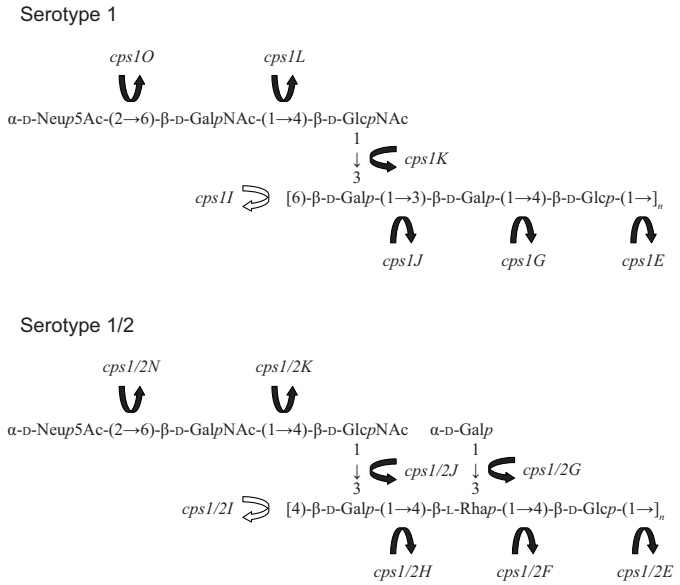

FIGURE 10. **Tentative correlation between structure and genes encoding enzymes responsible for the biosynthesis of *S. suis* CPSs.** *Black arrows*, glycosyltransferases; *white arrows*, polymerases.

example, antibodies against the side chain of serotype 1 CPS, which are mainly present in the anti-serotype 1 serum, do not recognize serotype 2 CPS side chain, but they seem to recognize serotype 14 CPS side chain. Because the serotype 2 and 14 CPS side chains are identical (Fig. 9), this observation can only be explained by a structural/conformational control of sialic acid in the serotype 2 CPS side chain, which is not observed in serotype 14, or related to structural/conformational control by the backbone (such as steric interactions with the α-Gal side chain). Nevertheless, homologous recognition of serotype 2 CPS by anti-serotype 2 serum is significantly reduced when sialic acid is removed in this serotype CPS (Fig. 8*C*). Thus, the side chain seems to dominate the antibody response generated by serotype 2 CPS. As mentioned previously, the lack of cross-reaction between anti-serotype 2 serum and serotype 1/2 desialylated polysaccharide further suggests low levels of anti-backbone antibodies generated by serotype 2 CPS. Finally, the enigmatic complete absence of recognition of serotype 2 CPS by serotype 1/2 antiserum highlights the complexity of the serotype 2 epitopes. It should be mentioned that our data only provided preliminary elucidation of the cross-reactions observed in *S. suis* serotyping, and structural/conformational characteristics of major CPS epitopes remain to be precisely determined by using, for example, a panel of monoclonal antibodies.

Based on structural and genetic homologies with serotypes 14 and 2, respectively, putative glycosyltransferase and polymerase genes in the *cps* loci of serotypes 1 and 1/2 were tentatively assigned to the transfer of specific sugars in the repeating units (supplemental Table S2 and Fig. 10). As mentioned previously, the only structural difference observed between serotype 2 and 1/2 CPSs and between serotype 1 and 14 CPSs is the sugar bearing the sialic acid in the side chains. The sugar is *N*-acetylgalactosamine in serotypes 1/2 and 1, whereas it is galactose in serotypes 2 and 14 (Fig. 9). The enzymes, which were assigned to the transfer of the sugars (Cps1L, Cps1/2K, Cps2K, and Cps14K), were classified into the same homology group (HG11) and annotated as a putative galactosyltransferase (9); however, if this tentative assignment is correct, Cps1L and Cps1/2K should function as an acetylgalactosaminyltransferase. To find sequence differences that may support this hypothesis, we retrieved amino acid sequences of Cps1L, Cps1/2K, Cps2K, and Cps14K from available databases and compared them. However, no sequence differences reasonably accounting for the possible change in function from a putative galactosyltransferase to a putative acetylgalactosaminyltransferase could be delineated from those published sequences (supplemental Fig. S12). In Fig. 10, we assigned *cps1G* (putative galactosyltransferase) to the transfer of galactose to the first glucose in the repeating unit. However, in a previous study (9), this gene was presumed to be a pseudogene due to a frameshift mutation at least in the serotype 1 reference strain and in a Chinese serotype 1 strain. To solve these discrepancies and confirm the precise function of each *cps* gene, further studies, including construction of gene-manipulated mutants and analysis of the CPS, are needed.

In conclusion, we generated for the first time data on CPS composition and structure that will contribute to understanding the cross-reactions observed in serotyping. The correct identification of the serotype may have public health impacts because, after serotype 2, serotype 14 is the type of *S. suis* most commonly isolated from human cases (1).

Author Contributions—M.-R. V. C. coordinated the structure determination portion of the study, analyzed the NMR spectra, and wrote the paper. G. G.-D. purified the CPS material, contributed to chemical analyses, and performed the lectin and serological tests. F. G. contributed to structure determination studies. All authors analyzed the results, contributed to manuscript writing and revision, and approved the final version of the manuscript.

Acknowledgments—We thank Adrien Brousse, Camille Soudier, and Nancy Guertin for technical assistance.

References

1. Goyette-Desjardins, G., Auger, J.-P., Xu, J., Segura, M., and Gottschalk, M. (2014) *Streptococcus suis*, an important pig pathogen and emerging zoonotic agent: an update on the worldwide distribution based on serotyping and sequence typing. *Emerg. Microbes Infect.* **3,** e45
2. Perch, B., Pedersen, K. B., and Henrichsen, J. (1983) Serology of capsulated streptococci pathogenic for pigs: six new serotypes of *Streptococcus suis*. *J. Clin. Microbiol.* **17,** 993–996
3. Gottschalk, M., Higgins, R., Jacques, M., Mittal, K. R., and Henrichsen, J. (1989) Description of 14 new capsular types of *Streptococcus suis*. *J. Clin. Microbiol.* **27,** 2633–2636
4. Gottschalk, M., Higgins, R., Jacques, M., Beaudoin, M., and Henrichsen, J. (1991) Characterization of six new capsular types (23 through 28) of *Streptococcus suis*. *J. Clin. Microbiol.* **29,** 2590–2594
5. Higgins, R., Gottschalk, M., Boudreau, M., Lebrun, A., and Henrichsen, J. (1995) Description of six new capsular types (29–34) of *Streptococcus suis*. *J. Vet. Diagn. Invest.* **7,** 405–406
6. Higgins, R., and Gottschalk, M. (1990) An update on *Streptococcus suis* identification. *J. Vet. Diagn. Invest.* **2,** 249–252
7. Perch, B., Kjems, E., Slot, P., and Pedersen, K. B. (1981) Biochemical and serological properties of R, S, and RS streptococci. *Acta Pathol. Microbiol. Scand. B* **89,** 167–171
8. Wang, K., Fan, W., Cai, L., Huang, B., and Lu, C. (2011) Genetic analysis of

the capsular polysaccharide synthesis locus in 15 *Streptococcus suis* serotypes. *FEMS Microbiol. Lett.* **324,** 117–124
9. Okura, M., Takamatsu, D., Maruyama, F., Nozawa, T., Nakagawa, I., Osaki, M., Sekizaki, T., Gottschalk, M., Kumagai, Y., and Hamada, S. (2013) Genetic analysis of capsular polysaccharide synthesis gene clusters from all serotypes of *Streptococcus suis*: potential mechanisms for generation of capsular variation. *Appl. Environ. Microbiol.* **79,** 2796–2806
10. Van Calsteren, M.-R., Gagnon, F., Calzas, C., Goyette-Desjardins, G., Okura, M., Takamatsu, D., Gottschalk, M., and Segura, M. (2013) Structure determination of *Streptococcus suis* serotype 14 capsular polysaccharide. *Biochem. Cell Biol.* **91,** 49–58
11. Van Calsteren, M.-R., Gagnon, F., Lacouture, S., Fittipaldi, N., and Gottschalk, M. (2010) Structure determination of *Streptococcus suis* serotype 2 capsular polysaccharide. *Biochem. Cell Biol.* **88,** 513–525
12. Shibuya, N., Goldstein, I. J., Broekaert, W. F., Nsimba-Lubaki, M., Peeters, B., and Peumans, W. J. (1987) The elderberry (*Sambucus nigra* L.) bark lectin recognizes the Neu5Ac(α2–6)Gal/GalNAc sequence. *J. Biol. Chem.* **262,** 1596–1601
13. Calzas, C., Goyette-Desjardins, G., Lemire, P., Gagnon, F., Lachance, C., Van Calsteren, M.-R., and Segura, M. (2013) Group B streptococcus and *Streptococcus suis* capsular polysaccharides induce chemokine production by dendritic cells via TLR2- and MyD88-dependent and -independent pathways. *Infect. Immun.* **81,** 3106–3118
14. Wishart, D. S., Bigam, C. G., Yao, J., Abildgaard, F., Dyson, H. J., Oldfield, E., Markley, J. L., and Sykes, B. D. (1995) ^{1}H, ^{13}C and ^{15}N chemical shift referencing in biomolecular NMR. *J. Biomol. NMR* **6,** 135–140
15. Zhu, G., and Bax, A. (1992) Improved linear prediction of damped NMR signals using modified "forward–backward" linear prediction. *J. Magn. Reson.* **100,** 202–207
16. Schneider, C. A., Rasband, W. S., and Eliceiri, K. W. (2012) NIH Image to ImageJ: 25 years of image analysis. *Nat. Methods* **9,** 671–675
17. Charland, N., Kellens, J. T. C., Caya, F., and Gottschalk, M. (1995) Agglutination of *Streptococcus suis* by sialic acid-binding lectins. *J. Clin. Microbiol.* **33,** 2220–2221
18. Carpita, N. C., and Shea, E. M. (1989) Linkage structure of carbohydrates by gas chromatography-mass spectrometry (GC-MS) of partially methylated alditol acetates. in *Analysis of Carbohydrates by GLC and MS* (Biermann, C. J., and McGinnis, G. D., eds) pp. 157–216, CRC Press, Inc., Boca Raton, FL
19. Machytka, D., Klein, R. A., and Egge, H. (1994) Reporter resonances in the NMR spectra of oligosaccharides containing sialic acid linked to galactopyranose rings. *Carbohydr. Res.* **254,** 289–294
20. Lundborg, M., and Widmalm, G. (2011) Structural analysis of glycans by NMR chemical shift prediction. *Anal. Chem.* **83,** 1514–1517
21. Lecours, M.-P., Fittipaldi, N., Takamatsu, D., Okura, M., Segura, M., Goyette-Desjardins, G., Van Calsteren, M.-R., and Gottschalk, M. (2012) Sialylation of *Streptococcus suis* serotype 2 is essential for capsule expression but is not responsible for the main capsular epitope. *Microbes Infect.* **14,** 941–950
22. Charland, N., Harel, J., Kobisch, M., Lacasse, S., and Gottschalk, M. (1998) *Streptococcus suis* serotype 2 mutants deficient in capsular expression. *Microbiology* **144,** 325–332
23. Smith, H. E., Damman, M., van der Velde, J., Wagenaar, F., Wisselink, H. J., Stockhofe-Zurwieden, N., and Smits, M. A. (1999) Identification and characterization of the *cps* locus of *Streptococcus suis* serotype 2: the capsule protects against phagocytosis and is an important virulence factor. *Infect. Immun.* **67,** 1750–1756
24. Roy, D., Auger, J.-P., Segura, M., Fittipaldi, N., Takamatsu, D., Okura, M., and Gottschalk, M. (2015) Role of the capsular polysaccharide as a virulence factor for *Streptococcus suis* serotype 14. *Can. J. Vet. Res.* **79,** 141–146
25. Chang, Y. C., and Nizet, V. (2014) The interplay between Siglecs and sialylated pathogens. *Glycobiology* **24,** 818–825
26. Elliott, S. D., and Tai, J. Y. (1978) The type-specific polysaccharides of *Streptococcus suis*. *J. Exp. Med.* **148,** 1699–1704
27. Cieslewicz, M. J., Chaffin, D., Glusman, G., Kasper, D., Madan, A., Rodrigues, S., Fahey, J., Wessels, M. R., and Rubens, C. E. (2005) Structural and genetic diversity of group B *Streptococcus* capsular polysaccharides. *Infect. Immun.* **73,** 3096–3103
28. Berti, F., Campisi, E., Toniolo, C., Morelli, L., Crotti, S., Rosini, R., Romano, M. R., Pinto, V., Brogioni, B., Torricelli, G., Janulczyk, R., Grandi, G., and Margarit, I. (2014) Structure of the type IX Group B *Streptococcus* capsular polysaccharide and its evolutionary relationship with types V and VI. *J. Biol. Chem.* **289,** 23437–23448
29. Segura, M., and Gottschalk, M. (2002) *Streptococcus suis* interactions with the murine macrophage cell line J774: adhesion and cytotoxicity. *Infect. Immun.* **70,** 4312–4322
30. Wang, Y., Gagnon, C. A., Savard, C., Music, N., Srednik, M., Segura, M., Lachance, C., Bellehumeur, C., and Gottschalk, M. (2013) Capsular sialic acid of *Streptococcus suis* serotype 2 binds to swine influenza virus and enhances bacterial interactions with virus-infected tracheal epithelial cells. *Infect. Immun.* **81,** 4498–4508
31. Wu, N. H., Meng, F., Seitz, M., Valentin-Weigand, P., and Herrler, G. (2015) Sialic acid-dependent interactions between influenza viruses and *Streptococcus suis* affect the infection of porcine tracheal cells. *J. Gen. Virol.* **96,** 2557–2568
32. Hough, L., Jones, J. V. S., and Wusteman, P. (1972) On the automated analysis of neutral monosaccharides in glycoproteins and polysaccharides. *Carbohydr. Res.* **21,** 9–17